RSC Advances

ROYAL SOCIETY OF CHEMISTRY

www.rsc.org/advances

The effect of electric field on hydrogen storage for B/N-codoped graphyne

Lihong Zhang[a], Ning Wang[a], Shengli Zhang[b], Shiping Huang*[a]

[a]State Key Laboratory of Organic-Inorganic Composites, Beijing University of Chemical Technology, Beijing 100029, China

[b]School of Materials Science and Engineering, Nanjing University of Science and Technology, Nanjing, Jiangsu, 210094, China

* Corresponding author: Fax: +86-10-64427616 E-mail: huangsp@mail.buct.edu.cn (S. Huang)

Abstract

Hydrogen adsorption on B/C/N sheet under different external electric fields is investigated by first-principles calculations. Through the analyses of structural properties of B/C/N system, we find that N_bB_f, B_bN_o, B_aN_e, and N_aB_g are more likely to be synthesized. Through molecular dynamics calculation, it is found that the structures for B/N doped graphyne are stable. For N_bB_f, B_bN_o, B_aN_e, and N_aB_g, the most stable positions for hydrogen adsorption are H1 sites. For a single H_2 adsorbed on B/C/N sheet, the adsorption energy increases greatly with the electric field increases, and the maximum adsorption energy is 0.506 eV when the electric field is 0.035 a.u. It is also found that the adsorption energy of H_2 adsorbed on N_bB_f under electric field increases faster than H_2 adsorbed on other sheets. The interaction between H_2 molecule and B/C/N sheet is Kubas interaction under an external electric field.

1. Introduction

Due to rising standards of living and growing of population, the energy consumption is expected to increase dramatically. Hydrogen is very attractive as a clean energy source because of its efficiency, abundance and environmental friendliness.[1–4] However, how to store hydrogen safely and transport efficiently is a crucial problem.[3,5]

Among various hydrogen storage materials, carbon-based nanostructures, including nanotubes[6], fullerenes[7] and graphenes, have attracted considerable attention because of their remarkable properties, such as good reversibility, high capacity, and fast kinetics.[8] However, hydrogen adsorption on carbon materials is limited by the van der Waals (vdW) interaction which is too weak to store hydrogen in moderate conditions. Recent studies showed that nanostructures composed of light elements such as B and N offer many advantages to store hydrogen.[9–11] For example, the BN layer is somewhat more resistant to oxidation than graphene, and thus more suitable for application at room temperature, where graphene would be oxidized.[12] Furthermore, similar to carbon nanotubes, BN nanotubes are also regarded as possible hydrogen storage media. It has been found experimentally that the BN nanotubes can store as much as 2.6 wt % of hydrogen at 10 MPa.[13] Collapsed BN nanotubes exhibit a higher hydrogen storage capacity with 4.2 wt % of hydrogen.[14] Moreover, Zhou et al. pointed that an effective method to promote hydrogen adsorption is to add external electric field.[9] The new concept is based on the fact that allows exposed metal cations to store hydrogen in quasi-molecular form is the polarization of the H_2 molecule

caused by the electric field associated with point ions.[15,16] Subsequently, Liu et al. put forward that electric field can induce a reversible switch for hydrogen adsorption and desorption based on Li-doped carbon nanotube and Li-doped graphene.[17,18] Enhanced hydrogen adsorption on carbonaceous sorbent under electric field has been demonstrated in experiment by Shi et al..[19]

Currently, there are some theoretical reports examining graphyne. Graphyne is a new carbon-based form that consists of planar carbon sheets containing sp and sp^2 bonds,[20–23] which can be regarded as the big hexagonal rings joined together by the acetylenic linkages (C-C≡C-C) rather than the C-C=C-C in graphene. In experiment, although large graphyne structures have not been synthesized yet, graphdiyne (expanded graphynes) films and graphdiyne tubes have been already obtained.[24]

In this study, we present theoretical study of the structure of 2D graphyne and their structural analogs involving BN rings (BN-yne). The latter is composed of BN hexagonal rings linked by C-chains. In this work, we investigate the stability of B/C/N systems, structural characteristic and electronic properties of hydrogen adsorption on B/C/N sheet using density functional theory (DFT) calculations. First, we study the possibility synthesize for B/C/N system based on the formation energy of B/C/N sheet. Then, we investigate stability of B/C/N sheet through dynamic calculation. Finally, we focus on the structural and electronic characteristics of hydrogen adsorption on B/C/N sheet under different electric fields.

2. Computational methods

All geometry optimizations are carried out using DFT calculations within the local density approximation (LDA) as implemented in the DMol3 package.[25,26] We apply the Perdew and Wang correlation functional (PWC)[27] and relax the geometries. Previous studies have demonstrated that LDA can predict the physisorption energies of H_2 on the surface of graphite and carbon nanotubes accurately[28–30] and can be suitable for charged carbon nanostructures with electric fields.[17,31] Full structural optimizations are obtained by using a convergence tolerance of energy of 1×10^{-5} Hartree, a maximum force of 2×10^{-3} Hartree/Å, and a maximum displacement of 5×10^{-3} Å. Moreover, a double numerical-polarized basis set (DNP) is employed. The DNP basis set include a double quality basis set with a p-type polarization function added to hydrogen and d-type polarization functions added to heavier atoms. Self-consistent field (SCF) calculations are performed with a convergence of 1×10^{-6} Hartree on the total energy. The direct inversion of iterative subspace (DIIS) approach is used to accelerate SCF convergence. A (2 × 2) B/N-codoped graphyne supercell is established, the lattice parameters are a = b = 13.7887 Å, c = 28.7497 Å, $\alpha = \beta = 90^{\circ}$, $\gamma = 120^{\circ}$. The vacuum space of 20 Å is used in the direction perpendicular to the B/C/N sheet in order to avoid the interaction between neighboring layers. The electric field is applied in the z direction, as shown in Fig. 1. The total density of states (DOS) and partial density of states (PDOS) of B/N-doped graphyne with and without electric field in the super cells are calculated with a k-point of (12 × 12 × 1). The Ortmann, Bechstedt and Schmidt (OBS) method is employed to correct the dispersion effect,[32]

and the effect of basis set superposition error (BSSE) is taken into account with the use of counterpoise (CP) correction.[33]

3. Results and discussion

The optimized structure of pristine graphyne is presented in Fig. 2. In pristine graphyne, the bonds of C atoms have three types, i.e., C-C single bond, C=C double bond, and C≡C triple bond (marked as number 1, 2, and 3 in Fig. 2, respectively). The bond lengths of C-C, C=C, and C≡C are 1.410 Å, 1.430 Å, and 1.227 Å, respectively. The calculated bond lengths are in good agreement with previously reports.[28,34] For B- or N-doped graphyne, there are two inequivalent sites for one B or N atom randomly substituting one C atom in graphyne, labeled as *a* and *b* in Fig. 2. After the structure optimization, the geometries are obtained and their structural parameters are presented in Table 1. The formation energy (E_F) can be defined as follows:

$$E_F = E_{DG} + n E_C - E_{PG} - \sum E_{Dopant} \quad (1)$$

where E_{DG} is the total energy of single doped or codoped graphyne, E_{PG} is the total energy of pristine graphyne, and $\sum E_{Dopant}$ is the total energy of dopant B, N, or B/N pairs. E_C is the energy of one carbon atom in pristine graphyne, and n is the number of carbon atom substituted by dopants. In the case of B doping at a site, the bond lengths of three B-C bonds are 1.528, 1.528, and 1.492 Å, longer than corresponding $d_{C\text{-}C}$ in pristine graphyne. For N doping, the bond lengths of three N-C bonds are 1.423, 1.423, and 1.357 Å, which are equal or shorter than corresponding $d_{C\text{-}C}$ in pristine graphyne. In the case of B (N) doping at b site, the bond lengths of B-C are 1.485 and

1.344 Å, longer than the corresponding $d_{C\text{-}C}$ in pristine graphyne; the bond lengths of N-C are 1.366 and 1.187 Å, shorter than the corresponding $d_{C\text{-}C}$ in pristine graphyne. In a word, the bond lengths of B-C (N-C) are longer (shorter) than the bond lengths of corresponding C-C bonds in the case of both B(N) doping at *a* site and *b* site, due to different atomic radius of B and N atoms. It can be seen from the formation energy (in Table 1) that B or N doped at *a* site and *b* site of graphyne are of great possibility to synthesize, especially for N-doped graphyne.

As for B/N codoping, we consider sixteen substitution sites. We divide the codoping configurations into two groups, as notated in Fig. 2. One is ax or xa (x = b, c, …, p) which represent that B (or N) atom substitutes C atom in a site and N (or B) atom substitutes C atom in b, c, d, e, f, g, h, i, j, k, l, m, n, o, and p sites, respectively; the other is by or yb (y = a, c, d, …, p) which indicate that B (or N) atom substitutes C atom in b site and N (or B) atom substitutes C atom in a, c, d, e, f, g, h, i, j, k, l, m, n, o, and p sites, respectively. As given in Table 2, the $d_{C\text{-}B}$ and $d_{C\text{-}N}$ for B/N codoping are almost the same as those of single B and N doping, indicating that the configuration keeps the planar structure.[35] The formation energies change from 0.190 to 0.265 eV for ax and from 0.150 to 0.233 eV for xa, indicating that N doping at a site is easier to synthesize than B doping at a site; the formation energies vary from 0.141 to 0.271 eV for bx and from 0.188 to 0.271 eV for xb, illuminating that B doping at b site is easier to synthesize than N doping at b site.

To check the stability of B/C/N system, we use the *ab* initio molecular dynamics (MD) simulation for B/C/N sheets. In the simulations, the temperature gradually

increases from 1 to 900 K in 1000 time steps, and the time step is 1 fs. It is found that the structure do not undergo an obvious deformation even at the temperature of 900 K.

Based on the formation energy, we choose four B/N-codoping configurations for example to investigate one H_2 adsorbed on different sites of B/C/N sheets. There are three types of adsorption sites on B/C/N sheets: hollow site (H), top site (T), and bridge site (B). For N_bB_f, there are two hollow sites, five top sites, and five bridge sites, as shown in Fig. 3(a). The calculated results of adsorption energies are summarized in Fig. 3(b). The adsorption energy of H_2 on B/C/N sheets is defined as follows:

$$E_{ad} = E^F_{B/C/N} + E^F_{H_2} - E^F_{H_2-B/C/N} \quad (2)$$

where $E_{H_2\text{-}B/C/N}$ is the total energy of H_2 adsorbed on B/C/N sheets, $E_{B/C/N}$ is the total energy of B/C/N sheets, and E_{H_2} is the total energy of free-standing H_2 molecule. F indicates the intensity of electric field, when $F = 0$, eq. 2 means the E_{ad} without the electric field; when $F \neq 0$, eq. 2 means the E_{ad} under the electric field. Dispersion and BSSE corrections are introduced to the calculation, and these correction data are listed in supporting information Table S1. It can be seen that the largest adsorption energy of H_2 adsorbed on N_bB_f is 0.407 eV at H1 site. Then, we calculate the adsorption energies of H_2 adsorbed on different sites of B_bN_o, B_aN_e, and N_aB_g sheets, the most favorable positions are also the H1 site with the largest adsorption energies of 0.400, 0.357, and 0.341 eV, respectively.

Then we study the relative stability of different configurations for H_2 molecule on

B/C/N sheet in an external electric field vertical to the sheet. As the same in the field-free case, three types of adsorption sites (top site, bridge site, and hollow site) are considered. For each site, various initial orientations of the H_2 molecule have been studied. After optimization, it can be seen that the angle between H_2 molecule and B/N-codoped graphyne plane increases with the increase of electric field, as shown in Fig. 4. And the H_2 molecule prefers to align along the z direction, i.e. parallel to the electric field, when the intensity of the electric field is strong enough, for example, 0.035 a.u. in the case of single H_2 absorbed on the N_bB_f sheet. For N_bB_f, B_bN_o, B_aN_e, and N_aB_g, the preferable positions are H1 sites; for N_a and N_b, the preferable positions are T4 and H2 sites.

We also investigate the effect of the electric field on hydrogen adsorption. As shown in Fig. 5, the hydrogen adsorption energy and the H-H bond length are plotted as a function of the magnitude of the electric field. Both dispersion and BSSE corrections are taken into account in the calculation, as listed in supporting information Table S2. It can be found that the adsorption energy increases dramatically under the electric field, indicating that the electric field can easily modulate the adsorption energy of H_2 adsorbed on B/C/N sheet. It is also found that the adsorption energy of H_2 adsorbed on N_bB_f under electric field increases faster than H_2 adsorbed on other sheets. Through Mulliken charge analysis in Table 3, we find that the charge of the B/C/N sheets increases with the electric field increasing, while the increase for electric quantity of N_bB_f is faster than other sheet. This may be account for why the adsorption energy of H_2 adsorbed on N_bB_f increases faster than

H_2 adsorbed on other sheets. Due to the polarization interaction induced by the electric field and the polar bonds on B/C/N sheets, the H-H bond length increase greatly with the electric filed increasing. When the electric field reaches 0.038 a.u., the H-H bond length becomes 0.870 Å for H_2 adsorbed on N_bB_f sheet, elongated nearly by 13%. It has been reported that the Kubas interaction between a transition metal atom and H_2 can elongate the bond length by 10-25%.[36,37] The interaction energy between H_2 molecule and B/N-codoped graphyne are in the range of 0.243 ~ 0.407 eV in absence of electric field. However, the interaction energy are in the range of 0.407 ~ 0.506 eV with electric field. These results illustrate the interaction between H_2 molecule and B/N-codoped graphyne is the Kubas interaction. From the analysis of molecular orbitals, it is found that the bonding orbitals are mainly between the π orbital of the B/N-codoped graphyne and the σ* anti-bonding orbital of the hydrogen molecule, and this interaction can be explained by the Kubas interaction.[35] When the electric field intensity is 0.039 a.u., we find that the H_2 molecule is dissociated. Therefore, the molecular hydrogen adsorption can be achieved only under a certain electric filed.

To investigate the effect of the electric field on the electronic structure, we analyses the partial density of states (PDOS) for a single H_2 adsorbed on B/C/N sheets under different electric fields. Fig. 6 shows the PDOS of the hydrogen atom, boron atom and nitrogen atom for H_2 adsorbed on N_bB_f. We find that the H-s orbital moves toward the Fermi level as the electric field increases. It indicates that the H_2 elongated by electric field is less stable than the free-H_2 molecule.

4. Conclusions

DFT calculations are carried out to explore B/C/N sheet for hydrogen storage. Through the analyses of structure for B/N-doped graphyne, it is found that N_bB_f, B_bN_o, B_aN_e, and N_aB_g are more likely to synthesize. For N_bB_f, after a single H_2 adsorption, it is found that the adsorption energy is 0.41 eV. In order to enhance the adsorption energy of H_2, a vertical electric field is applied on B/C/N sheet. It is shown that the H_2 molecule is polarized under an external electric field. It can be seen that the adsorption energy increases dramatically with the increase of electric field intensity. The bond length of H-H increases as the electric field increases within a certain range. The hydrogen molecules are not dissociated and are all stored in molecular form.

Acknowledgments

This work is supported by the National Natural Science Foundation of China (Grant 21376013).

References

1 J. Alper, *Science*, 2003, **299**, 1686–1687.

2 R. D. Cortright, R. R. Davda and J. A. Dumesic, *Nature*, 2002, **418**, 964–967.

3 L. Schlapbach and A. Züttel, *Nature***,** 2001, **414**, 353–358.

4 Y. Lu, R. Jin and W. Chen, *Nanoscale*, 2011, **3**, 2476–2480.

5 R. Coontz and B. Hanson, *Science*, 2004, **305**, 957.

6 C. Liu, Y. Y. Fan, M. Liu, H. T. Cong, H. M. Cheng and M. S. Dresselhaus, *Science*, 1999, **286**, 1127–1129.

7 H. Kruse and S. Grimme, *J. Phys. Chem. C*, 2009, **113**, 17006–17010.

8 A. C. Dillon and M. J. Heben, *Appl. Phys. A: Mater. Sci. Process.*, 2001, **72**, 133–142.

9 J. Zhou, Q. Wang, Q. Sun, P. Jena and X. S. Chen, *Proc. Natl. Acad. Sci.*, 2010, **107**, 2801–2806.

10 M. Khazaei, M. S. Bahramy, N. S. Venkataramanan, H. Mizuseki and Y. Kawazoe, *J. Appl. Phys.*, 2009, **106**, 094303.

11 L. P. Zhang, P. Wu and M. B. Sullivan, *J. Phys. Chem. C*, 2011, **115**, 4289–4296.

12 J. Wang, C. H. Lee and Y. K. Yap, *Nanoscale*, 2010, **2**, 2028–2034.

13 R. Ma, Y. Bando, H. Zhu, T. Sato, C. Xu and D. Wu, *J. Am. Chem. Soc.*, 2002, **124**, 7672–7673.

14 C. C. Tang, Y. Bando, T. Sato, K. Kurashima, X. X. Ding, Z. W. Gan and S. R. Qi, *Appl. Phys. Lett.*, 2002, **80**, 4641–4643.

15 J. Niu, B. K. Rao and P. Jena, *Phys. Rev. Lett.*, 1992, **68**, 2277.

16 M. Yoon, S. Yang, C. Hicke, E. Wang, D. Geohegan and Z. Zhang, *Phys. Rev. Lett.*, 2008, **100**, 206806.

17 W. Liu, Y. H. Zhao, J. Nguyen, Y. Li, Q. Jiang and E. J. Lavernia, *Carbon*, 2009, **47**, 3452–3460.

18 W. Liu, Y. H. Zhao, Y. Li, Q. Jiang and E. J. Lavernia, *J. Phys. Chem. C*, 2009, **113**, 2028–2033.

19 S. Shi, J. Y. Hwang, X. Li, X. Sun and B. I. Lee, *Int. J. Hydrogen Energy*, 2010, **35**, 629–631.

20 R. H. Baughman, H. Eckhardt and M. Kertesz, *J. Chem. Phys.*, 1987, **87**, 6687–6699.

21 N. Narita, S. Nagai, S. Suzuki and K. Nakao, *Phys. Rev. B*, 1998, **58**, 11009.

22 L. D. Pan, L. Z. Zhang, B. Q. Song, S. X. Du and H. J. Gao, *Appl. Phys. Lett.*, 2011, **98**, 173102.

23 M. Long, L. Tang, D. Wang, Y. Li and Z. Shuai, *ACS Nano*, 2011, **5**, 2593–2600.

24 G. Li, Y. Li, H. Liu, Y. Guo, Y. Li and D. Zhu, *Chem. Commun.*, 2010, **46**, 3256–3258.

25 B. Delley, *J. Chem. Phys.*, 1990, **92**, 508–517.

26 B. Delley, *J. Chem. Phys.*, 2000, **113**, 7756–7764.

27 J. P. Perdew and Y. Wang, *Phys. Rev. B: Condens. Matter Mater. Phys.*, 1992, **45**, 13244–13249.

28 Y. Okamoto and Y. Miyamoto, *J. Phys. Chem. B*, 2001, **105**, 3470–3474.

29 J. I. Martínez, I. Cabria, M. J. López and J. A. Alonso, *J. Phys. Chem. C*, 2009, **113**, 939–941.

30 Z. M. Ao, Q. Jiang, R. Q. Zhang, T. T. Tan and S. Li, *J. Appl. Phys.*, 2009, **105**, 074307.

31 Y. V. Shtogun and L. M. Woods, *J. Phys. Chem. C*, 2009, **113**, 4792–4796.

32 F. Ortmann, F. Bechstedt and W. G. Schmidt, *Phys. Rev. B: Condens. Matter Mater. Phys.*, 2006, **73**, 205101.

33 S. F. Boys and F. Bernardi, *Mol. Phys.*, 1970, **19**, 553-566.

34 I. Cabria, M. J. López and J. A. Alonso, *J. Chem. Phys.*, 2008, **128**, 144704.

35 X. Deng, M. Si and J. Dai, *J. Chem. Phys.*, 2012, **137**, 201101.

36 B. Kiran, A. K. Kandalam and P. Jena, *J. Chem. Phys.*, 2006, **124**, 224703.

37 J. H. Guo, W. D. Wu and H. Zhang, *Struct. Chem.*, 2009, **20**, 1107–1113.

Table 1 The bond lengths of C-B (C-N), and the formation energies E_F for B or N doping.

	B doping		N doping	
	a site	b site	a site	b site
$d_{C\text{-}B(N)}$ (Å)	1.528, 1.492	1.485, 1.344	1.423, 1.357	1.366, 1.187
E_F (eV)	0.23	0.19	0.15	0.19

Table 2 The C-dopants distance ($d_{C\text{-}B}$ and $d_{C\text{-}N}$), and the formation energy (E_F). When B or N atom bind with several C atoms, the $d_{C\text{-}B}$ or $d_{C\text{-}N}$ indicate the shortest bond length. (The definitions of all symbols can be seen in Fig.2).

ax	*ab*	*ac*	*ad*	*ae*	*af*	*ag*	*ah*	*ai*	*aj*	*ak*	*al*	*am*	*an*	*ao*	*ap*
$d_{C\text{-}B}$(Å)	1.521	1.512	1.504	1.497	1.490	1.490	1.488	1.491	1.489	1.488	1.491	1.492	1.493	1.492	1.494
$d_{C\text{-}N}$ (Å)	1.179	1.172	1.344	1.355	1.187	1.186	1.355	1.348	1.185	1.179	1.352	1.406	1.405	1.415	1.405
E_F (eV)	0.265	0.237	0.196	0.190	0.228	0.227	0.193	0.191	0.240	0.235	0.233	0.233	0.196	0.200	0.197
xa	*ba*	*ca*	*da*	*ea*	*fa*	*ga*	*ha*	*ia*	*ja*	*ka*	*la*	*ma*	*na*	*oa*	*pa*
$d_{C\text{-}B}$ (Å)	1.348	1.342	1.504	1.490	1.346	1.345	1.489	1.495	1.346	1.343	1.490	1.526	1.521	1.526	1.520
$d_{C\text{-}N}$ (Å)	1.415	1.315	1.344	1.348	1.354	1.353	1.355	1.354	1.352	1.355	1.352	1.353	1.355	1.350	1.354
E_F (eV)	0.189	0.156	0.196	0.191	0.152	0.150	0.193	0.190	0.162	0.153	0.232	0.233	0.196	0.200	0.196

by	*ba*	*bc*	*bd*	*be*	*bf*	*bg*	*bh*	*bi*	*bj*	*bk*	*bl*	*bm*	*bn*	*bo*	*bp*
$d_{C\text{-}B}$ (Å)	1.348	1.513	1.342	1.347	1.344	1.344	1.345	1.346	1.342	1.344	1.343	1.343	1.348	1.351	1.348
$d_{C\text{-}N}$ (Å)	1.415	1.337	1.315	1.352	1.185	1.187	1.352	1.354	1.187	1.187	1.355	1.411	1.416	1.425	1.417
E_F (eV)	0.189	0.271	0.156	0.162	0.190	0.192	0.150	0.152	0.188	0.189	0.153	0.153	0.153	0.141	0.153

yb	*ab*	*cb*	*db*	*eb*	*fb*	*gb*	*hb*	*ib*	*jb*	*kb*	*lb*	*mb*	*nb*	*ob*	*pb*
$d_{C\text{-}B}$ (Å)	1.521	1.512	1.514	1.488	1.343	1.344	1.490	1.490	1.344	1.344	1.487	1.527	1.532	1.531	1.530
$d_{C\text{-}N}$ (Å)	1.179	1.337	1.173	1.184	1.187	1.187	1.186	1.188	1.185	1.187	1.180	1.179	1.182	1.175	1.182
E_F (eV)	0.265	0.271	0.237	0.240	0.188	0.192	0.227	0.228	0.190	0.189	0.234	0.235	0.230	0.222	0.230

Table 3 The change of Mulliken charge for B/C/N sheets under the electric field.

E-field (a.u.)	The Mulliken charge for B/C/N sheets (|e|)			
	B_bN_o	B_aN_e	N_aB_g	N_bB_f
0	0.012	0.010	0.007	0.010
0.02	0.049	0.026	0.044	0.048
0.035	0.143	0.077	0.143	0.155

Figure Captions

Fig. 1 Single H_2 adsorbed on the N_bB_f sheet, vertical electric field is applied in the z direction.

Fig. 2 The optimized structure of pristine graphyne. Numbers 1, 2, and 3 donate C-C, C=C, and C≡C bonds, respectively; Letters *a, b, ..., p* represent 16 substitution positions for B(N) doping and B/N codoping.

Fig. 3 (a) Different adsorption sites on N_bB_f sheet, including two hollow sits (H), five top sites (T), and five bridge sites (B). The gray, blue, and yellow balls are carbon, nitrogen, and boron atoms, respectively. (b) The adsorption energy of H_2 adsorbed on different sites of N_bB_f sheet with DFT-D and BSSE correction.

Fig. 4 The configurations of single H_2 absorbed on the N_bB_f sheet, with the increase of electric field. The vertical coordinate represents the angle between H_2 molecule and B/N-codoped graphyne plane.

Fig. 5 (a) The adsorption energy (b) The H-H bond length as a function of the magnitude of the electric field.

Fig. 6 The partial density of states for one single H_2 adsorbed on N_bB_f under different electric fields. (a) The electric field is 0.000 a.u. (b) The electric field is 0.020 a.u. (c) The electric field is 0.038 a.u. The Fermi energy is set to zero.

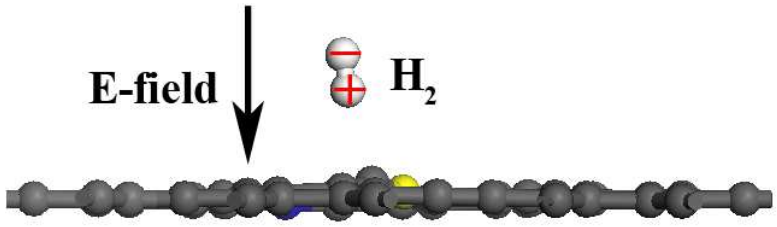

Fig. 1 Single H_2 adsorbed on the N_bB_f sheet, vertical electric field is applied in the z direction.

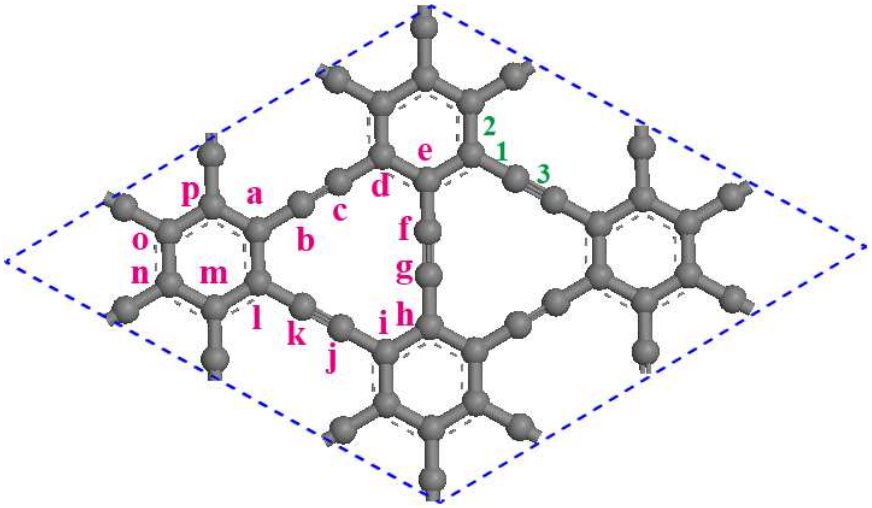

Fig. 2 The optimized structure of pristine graphyne. Numbers 1, 2, and 3 donate C-C, C=C, and C≡C bonds, respectively; Letters *a, b, ..., p* represent 16 substitution positions for B(N) doping and B/N codoping.

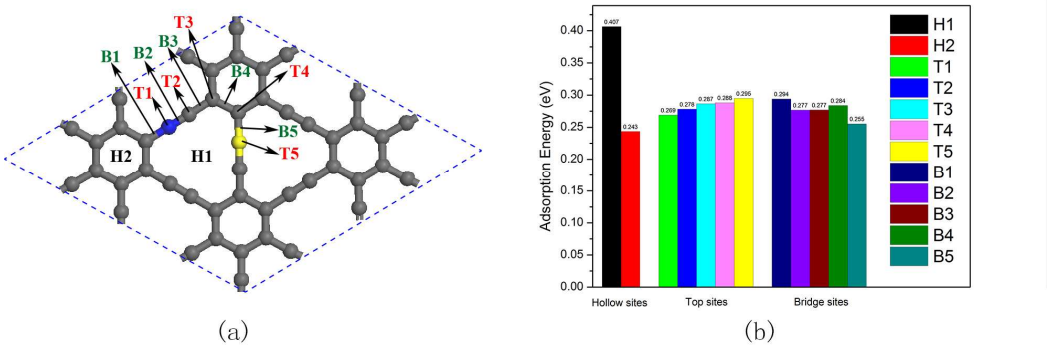

Fig. 3 (a) Different adsorption sites on N_bB_f sheet, including two hollow sites (H), five top sites (T), and five bridge sites (B). The gray, blue, and yellow balls are carbon, nitrogen, and boron atoms, respectively. (b) The adsorption energy of H_2 adsorbed on different sites of N_bB_f sheet with DFT-D and BSSE correction.

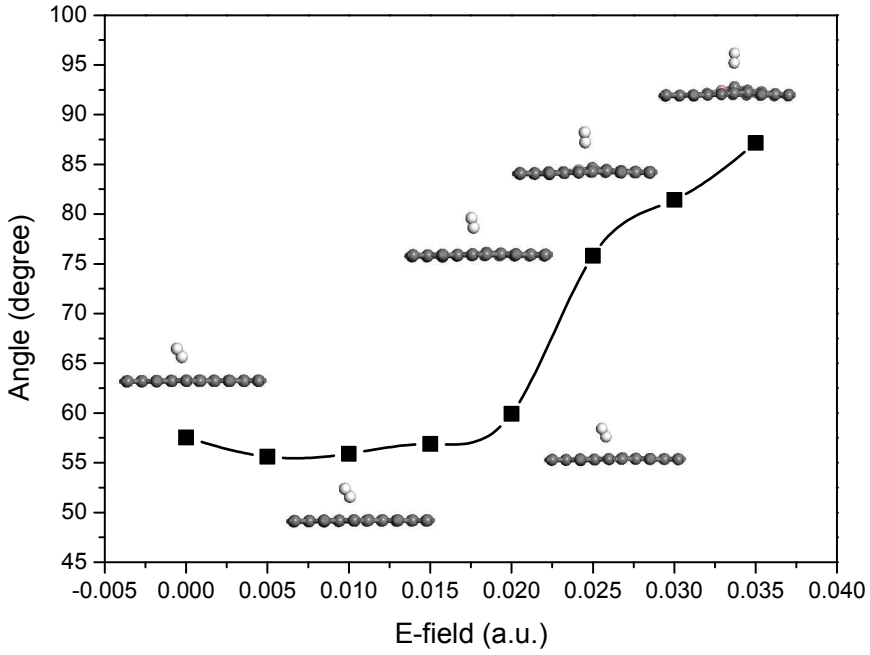

Fig. 4 The configurations of single H_2 absorbed on the N_bB_f sheet, with the increase of electric field. The vertical coordinate represents the angle between H_2 molecule and B/N-codoped graphyne plane.

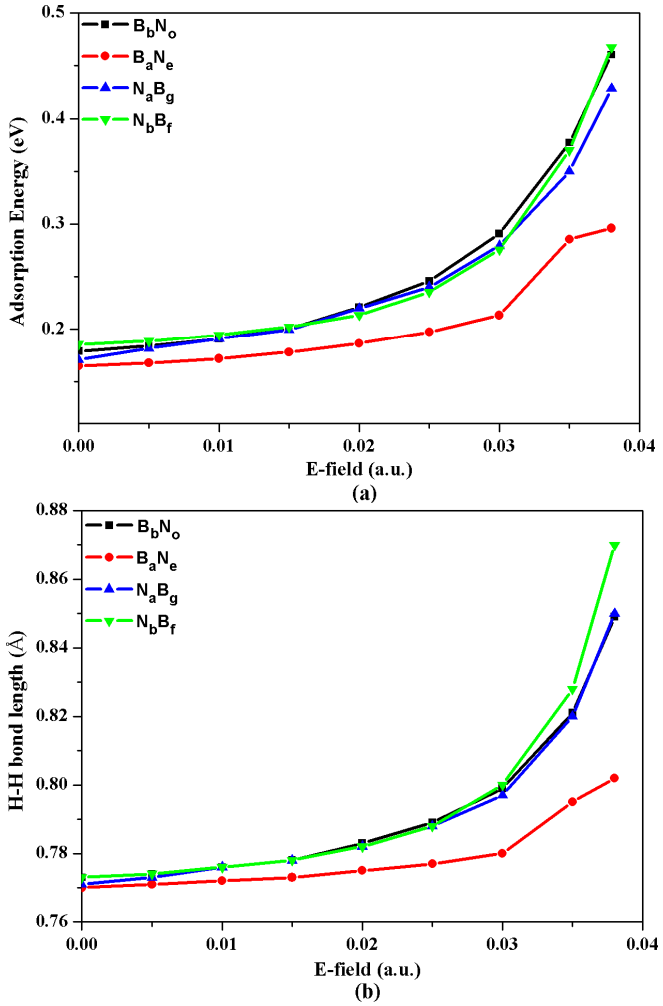

Fig. 5 (a) The adsorption energy (b) The H-H bond length as a function of the magnitude of the electric field.

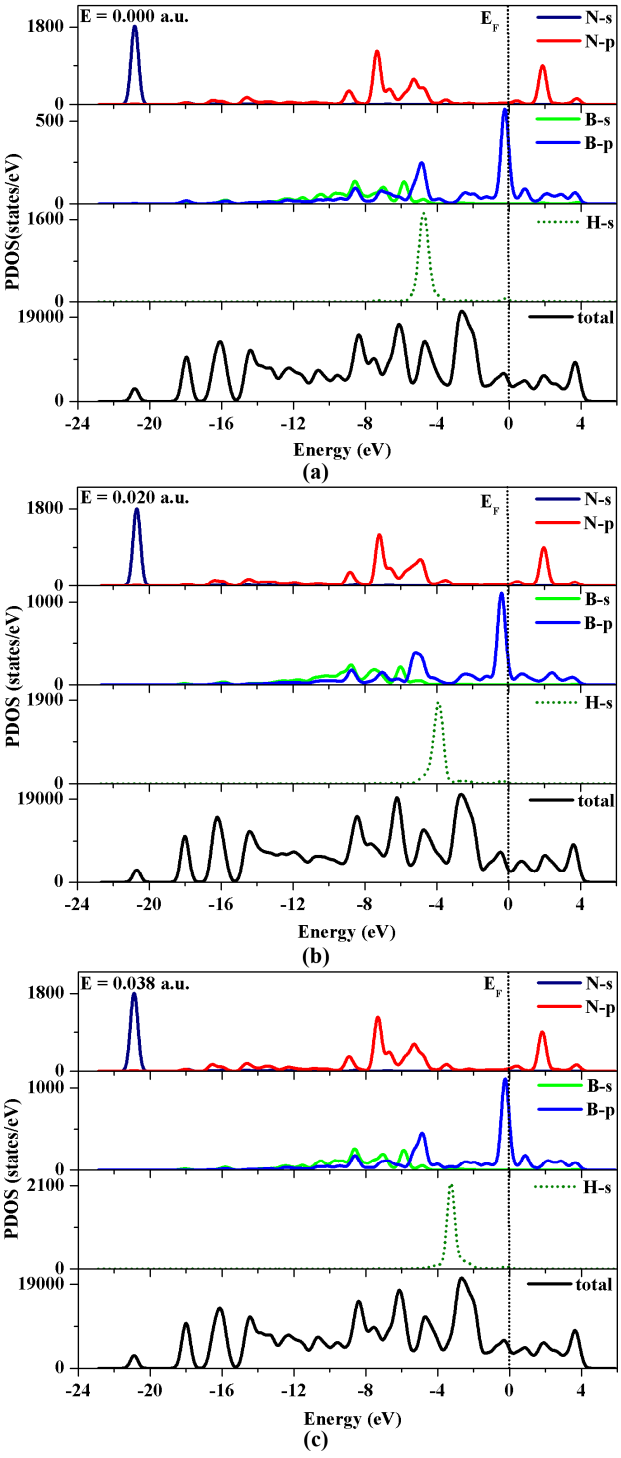

Fig. 6 The partial density of states for one single H_2 adsorbed on N_bB_f under different electric fields. (a) The electric field is 0.000 a.u. (b) The electric field is 0.020 a.u. (c) The electric field is 0.038 a.u. The Fermi energy is set to zero.

Table of contents

The interaction between H_2 molecule and B/C/N sheet is Kubas interaction under an external electric field.